Proc. 3rd International Conference on Networked Sensing Systems (INSS 2006), pp. 55-60, Rosemont, Illinois (USA), May, 2006.

A Whole Body Artificial Skin Based on Cell-Bridge Networking System

Takayuki Hoshi, Akimasa Okada, Yasutoshi Makino, and Hiroyuki Shinoda
Department of Information Physics and Computing
Graduate School of Information Science and Technology, The University of Tokyo
Tokyo, Japan
{star, okada, yasutoc, shino}@alab.t.u-tokyo.ac.jp

***Abstract*—We proposed a novel communication system named "cell-bridge system" for sensor networks in the previous INSS workshop. The system consists of two dimensional areas called "cells" and signal transmission devices called "bridges". In this paper, we propose a tactile sensor skin as one of applications of the system. In this application, the cells are not only communication media but also parts of capacitive tactile sensor elements, and the bridges not only transmit signals but also measure the capacitances of the sensor elements. The structure of the sensor element is very simple; two layers of compressible insulators which are sandwiched between three pieces of stretchable conductive sheets. The sensor element acquires a contact area in addition to a contact force within its sensing area. The resulting robot skin is soft, stretchable, and able to cover a large area such as a whole surface of a humanoid robot.**

Keywords-cell bridge; robot skin; sensor network; tactile sensor

I. INTRODUCTION

In these years, there is a growing interest in home robots that can care for the aged and young children [1][2] and that can be alternatives to companion animals [3][4]. In that situation, robots in home are required to be more cautious about surrounding environments than robots in industrial factories because they interact with humans directly and there are obstacles and unpredictable events around them. To meet this requisite, robot skins which give tactile sensation to the robots are demanded in robotics [5].

The major requirements for robot skins are as follows.

- They should sensitively detect rich tactile information related to such parameters as shape, pressure, friction, temperature, and so on.
- They should cover several-square-meter large areas such as whole surfaces of robots.
- They should be soft and stretchable to contact humans safely and fit robot surfaces. Softness is one of important factors to detect touch feelings, too.

To fill these requirements, robot skins are ordinarily designed as arrays of pressure-sensitive tactile sensor elements [6]-[11]. One widely used method is linking the tactile sensor elements to a host computer or a measurement circuit by hard long wires. In this method, softness of resulting robot skins is lost because of the wires. The radio technology seems to be a solution for it [12]. But there are many cases in which the wireless method is impractical in terms of the energy consumption, the power supply, and the acquired throughput.

To solve those problems, we proposed a novel signal transmission system in which the network is constructed by "cells" and "bridges" [13]. The bridge is a communication chip that can transmit and receive electric signals. The cell is a two-dimensional medium through which the bridges exchange signals each other. Many kinds of such materials as conductive rubber or fabric are available for it. By connecting sensor elements to the cells, we can realize a high-density sensor network. Furthermore, the cell-bridge system is effective when the cells are given additional function of sensor or actuator. For example, the cells are given the function of electrostatic speaker in [14].

In this paper, we apply this system to a robot skin (Fig. 1). The cells are also components of our tactile sensor elements proposed in [15]. The sensor element has a several-square-centimeter large sensing area and acquires not only a contact force but also a contact area using the nonlinear elasticity.

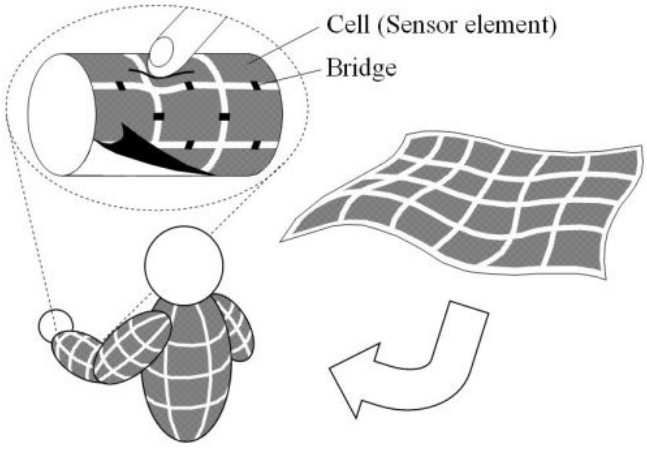

Figure 1. Proposed tactile sensor skin based on cell-bridge system. It is soft, stretchable, and capable of covering a large area.

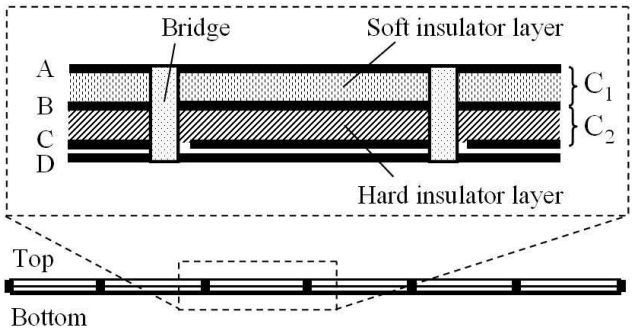

Figure 2. Cross-section of sensor skin. A: Ground layer, B: Sensor/Cell layer, C: Sensor layer, and D: Power layer. A set of soft and hard insulator layers and three pieces of conductive layers A, B, and C form one sensor element.

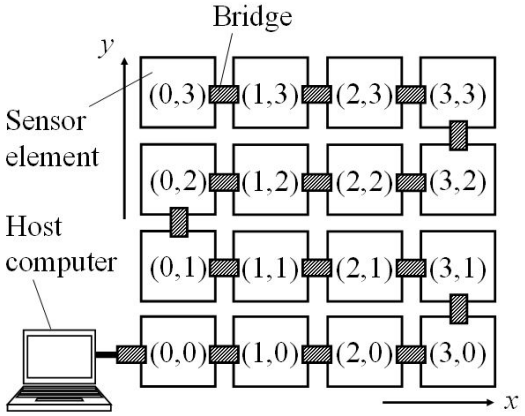

Figure 3. Scheme of sensor skin. Each sensor element has its specific coordinate. The sensor elements are linked in a row by the bridges. The element with the coordinate (0, 3) is the most upstream, and the element with (0, 0) is the most downstream connected to the host computer.

Owing to the additional sensing parameter, i.e. the contact area, a robot skin which detects minute shape features is easily realized by arraying the elements in low density. In consequence, we can cover whole surfaces of robots with a small number of the elements. This proposition is inspired by the characteristics of the human tactile sensation. While Two Point Discrimination Thresholds (TPDT) of humans are as large as several centimeters except on especially sensitive parts, faces and hands [16], sharpness of objects can be discriminated sensitively even on such large TPDT parts. From these facts, we suppose that sharpness is one of key components to produce general human tactile sensation [17], and that sensitivity to sharpness is a high priority for human-like sensor skins.

The rest of this paper is organized as follows. Firstly, Section II describes the structure of the proposed tactile sensor skin. After that, we explain the sensor element in Section III, and the bridge in Section IV. Finally, we conclude this paper in Section V.

II. Structure of Tactile Sensor Skin

We propose a new tactile sensor skin based on the cell-bridge system. The cross-section of the sensor skin is shown in Fig. 2. There are two compressible insulator layers which have different stiffness and a thin stretchable insulator layer. Besides, there are four stretchable conductive layers; the conductive layers A, B, C, and D are the ground layer, the sensor/cell layer, the other sensor layer, and the power layer, respectively. The conductive layers A and B sandwich the soft insulator layer forming the capacitor named C_1, and B and C sandwich the hard insulator layer forming C_2. This pair of the capacitors is one tactile sensor element. The conductive layers C and D are isolated by the thin stretchable insulator layer. The bridge is mounted in the structure and connected with the conductive layers. It is supplied power from the layers A and D (the ground and power layers). These two layers also function as electrostatic shields. It measures the capacitances C_n [F] (n = 1, 2) and sends measured data to the host computer through the conductive layer B (the cell layer) by multi-hoping method. The structure described here can maintain the softness of the sensor skin because it contains no long wires.

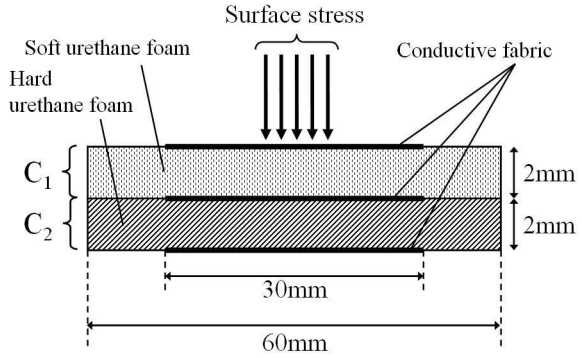

Figure 4. Cross-section of prototype of one tactile sensor element.

The scheme of the sensor skin system is illustrated in Fig. 3. The system consists of the arrayed sensor elements and the bridges arranged at the boundaries of the sensor elements. While we will arrange the bridges at all four sides of the sensor elements in future, we now link the elements in a row for simplicity of the protocol. Each sensor element has its specific coordinate as shown in Fig. 3. The element with the coordinate (0, 3) is the most upstream, and the element with (0, 0) is the most downstream connected to the host computer. While the number of the sensor elements is only 16 in the current version, additional elements could be linked in the same manner.

III. Tactile Sensor Element

A. Structure

The structure of our sensor element is very simple. In Fig. 4, we show schematically the cross-section of the sensor element prototype. The sensor element consists of two insulator layers; the upper and lower layers are soft (15 kg/m^3) and hard (60 kg/m^3) urethane foam, respectively, and each layer is 2 mm in thickness. There are three pieces of stretchable conductive fabric on the soft layer, between the soft and hard, and under the hard. Each piece has an area of 30×30 mm^2. The side length of the conductive fabric piece is comparable to the TPDT on human forearms. The insulator layers and the conductive pieces

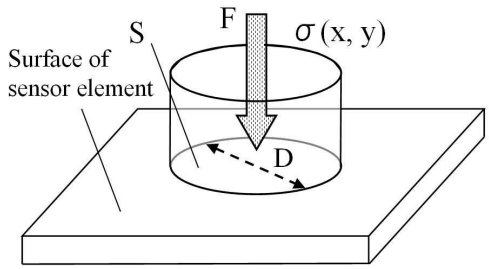

Figure 5. Supposed surface stress distribution $\sigma(x, y)$.

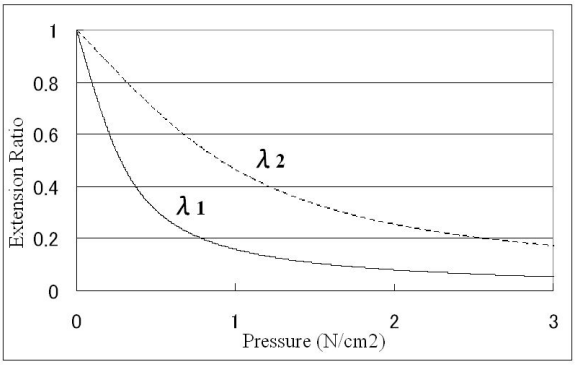

Figure 6. Relationship between surface stress σ and extension ratio λ_n. The soft layer λ_1 is more easily compressed than the hard layer λ_2.

adhere to each other by soft double-faced tape, and two capacitors are formed in the layers. Supposing a surface of a robot body hard, we attach the bottom of the sensor element prototype to an acrylic base.

B. Sensing Theory

We suppose a surface stress distribution as illustrated in Fig. 5; a constant surface stress distribution $\sigma(x, y)$ [Pa] is vertically loaded to the surface of the sensor element in a contact field S, that is,

$$\sigma(x, y) \equiv \begin{cases} F / S & \text{if } (x, y) \in \mathrm{S} \\ 0 & \text{if } (x, y) \notin \mathrm{S} \end{cases} \tag{1}$$

where F [N] is the total intensity of the contact force and S [m^2] is the area of S. Now we take note of the area of S, not the shape, so we suppose that S is circular for simplicity.

We also assume as follows. First, the nonlinear elasticity of the insulator layers is the entropy elasticity [18] expressed as

$$\sigma = \frac{E_n}{3}\left(\frac{1}{\lambda_n} - \lambda_n^2\right) \quad (n = 1, 2) \tag{2}$$

$$\lambda_n \equiv 1 - \Delta d_n / d_n \tag{3}$$

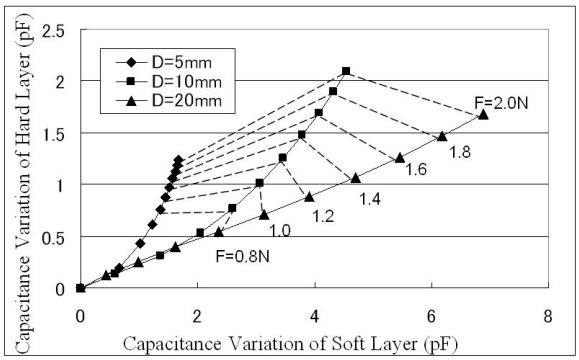

Figure 7. Simulation result. Calculated (ΔC_1, ΔC_2)s for various (F, S)s. D is the diameter of S for a circular object.

where n is the layer identification; n = 1 means the upper soft layer and 2 the lower hard layer. E_n [Pa], λ_n and d_n [m] are the elasticity modulus, the extension ratio and the initial thickness of the layer n, respectively. E_1 is about 4.8 kPa and E_2 is 15 kPa by actual measurement. The following expression of λ_n (Fig. 6) is obtained by solving (2),

$$\lambda_n = \sqrt[3]{\frac{1}{2} + \sqrt{\frac{1}{4} + \left(\frac{\sigma}{E_n}\right)^3}} + \sqrt[3]{\frac{1}{2} - \sqrt{\frac{1}{4} + \left(\frac{\sigma}{E_n}\right)^3}} \,. \tag{4}$$

Second, the conductive pieces have negligible tensions and the Poisson's ratios of the insulator layers are zero, which means that a displacement distribution $\Delta d_n(x, y)$ [m] is determined simply by the local value of $\sigma(x, y)$. We measure electric capacitances C_n [F] between the conductive pieces to detect $\Delta d_n(x, y)$. Ignoring fringing fields, the capacitance is formulated as

$$C_n = \iint_{\text{Element}} \frac{\varepsilon_n}{d_n - \Delta d_n(x, y)} \mathrm{d}x\mathrm{d}y \tag{5}$$

where ε_n [F/m] is the dielectric constant of the layer n. If we can make the second assumption mentioned above, (C_1, C_2) is uniquely determined by (F, S). Then the key question is whether the inverse mapping from (C_1, C_2) to (F, S) is possible or not for the layers 1 and 2 having different hardness.

Fig. 7 shows a numerical simulation result for the elasticity moduli E_1 = 4.8 kPa and E_2 = 15 kPa. It shows that the plot of (ΔC_1, ΔC_2)s for various (F, S)s spans a two dimensional space, where (ΔC_1, ΔC_2) are the capacitance variations by the applied force, and D is a parameter defined as

$$D \equiv 2\sqrt{S / \pi} \tag{6}$$

to represent the diameter of S for a circular object. It implies that we can determine (F, S) uniquely from (ΔC_1, ΔC_2) when F is larger than a threshold, now around 1.0 N.

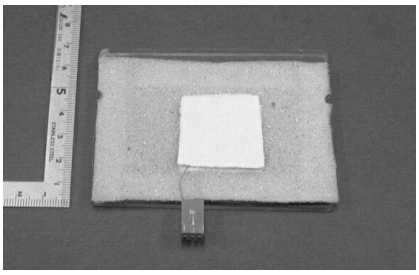

Figure 8. Photograph of sensor element prototype.

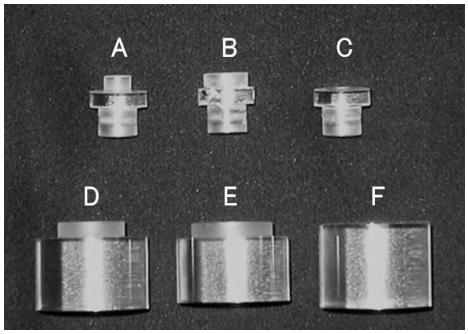

Figure 9. Acrylic stimulators used in experiment. A: D = 10 mm, B: D = 16 mm, C: D = 20 mm, D: D = 26 mm, E: D = 30 mm, and F: D = 40 mm.

Note that the nonlinear elasticity of the insulator layers plays a key role in the sensing theory. In the case of linear elastic insulator layers, i.e. $\sigma << E_n$, it is impossible to estimate S from (C_1, C_2). λ_n of the linear elastic insulator is calculated by approximating (4) as

$$\lambda_n \cong 1 - \sigma / E_n \,. \tag{7}$$

Then (5) can be approximated as

$$C_n \cong C_{n0} + \varepsilon_n F / d_n E_n \tag{8}$$

where C_{n0} is the initial capacitance of the layer n. Equation (8) means that neither C_1 nor C_2 contains the parameter S.

C. Experiment and Result

We conducted an experiment to examine the feasibility of the proposed sensing method. We measured C_n of the sensor element prototype (Fig. 8) by a self oscillation method; we generated a RC oscillation including the sensor element as the capacitor, and counted pulses par 2 ms by a 16-bit counter. A PC imported data via a digital I/O, and achieved around 80 Hz effective sampling rate. We used six acrylic stimulators with diameters D = 10, 16, 20, 26, 30, and 40 mm (Fig. 9). Each stimulator was vertically pressed at the center of the sensor element. It was operated quasi-statically by a mechanical z-stage, with measuring the pressing force F by a weighting machine.

Fig. 10 shows how (F, S)s are represented in the (ΔC_1, ΔC_2) space. It is confirmed that the plot of (ΔC_1, ΔC_2)s spans a two

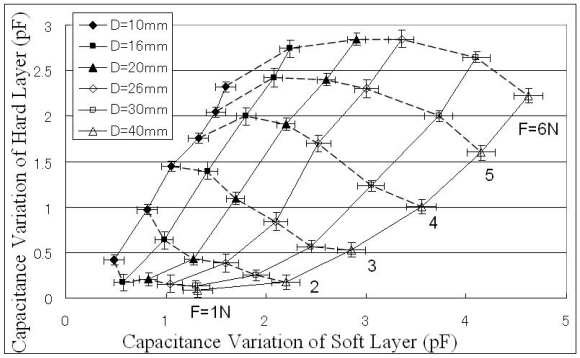

Figure 10. Experimental result of 5 trials. Averaged trajectories of (ΔC_1, ΔC_2)s for various (F, S)s with error bars representing maximal deviations.

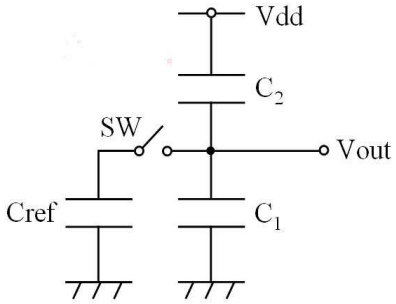

Figure 11. Equivalent circuit of measurement system.

dimensional space sufficiently. The reason of the quantitative difference from the simulation result (Fig. 7) is considered to be the tension of the actual conductive fabric.

IV. BRIDGE

A. Packets and Operations

In the current version of the protocol, two kinds of packets, the data packet and the command packet are employed. The packets are transmitted downstream (see Fig. 3). The data packet contains the measured data and the coordinate of the sensor element, and the command packet contains the cue signal for the next bridge to measure the capacitances of the sensor element.

The bridge is standby when there is no packet. In receiving the data packet, the bridge transfers the identical packet to the downstream bridge through the cell layer. On the other hand, in receiving the command packet, the bridge executes the following two-step sequence. Firstly, the bridge measures the capacitances C_n and sends the data packet containing the measured data to the downstream bridge through the cell layer. Next, the bridge generates and sends the command packet to the downstream bridge. By the iteration of this process, the host computer can gather the data from the all sensor elements.

The most upstream bridge connected to the sensor element with the coordinate (0, 3) alone executes the above sequence spontaneously at adequate intervals without waiting for the command packet.

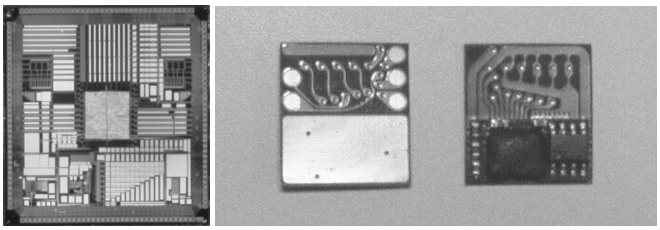

(a) (b)

Figure 12. (a) Closeup top view of first prototype of CMOS LSI (5×5 mm^2). (b) LSI packaged on flexible substrate (16×18 mm^2, opened).

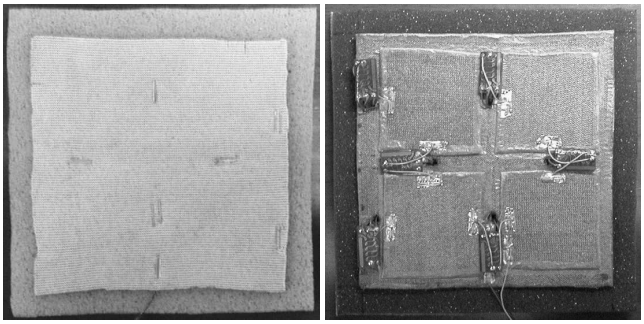

(a) (b)

Figure 13. Developed 2×2 tactile sensor array. Each sensor element is 40×40 mm^2. (a) and (b) are top and bottom views of the test model.

B. Capacitance Measurement

Fig. 11 shows the equivalent circuit of the measurement system. There is a reference capacitor Cref inside the bridge connected through a switch SW to the junction of the capacitors C_1 and C_2. The bridge measures the divided voltage *Vout* between the power voltage *Vdd* and the ground voltage. The divided voltages are represented as

$$Vout(\mathrm{OFF}) = \frac{C_2}{C_1 + C_2} Vdd \tag{9}$$

$$Vout(\mathrm{ON}) = \frac{C_2}{C_1 + C_2 + Cref} Vdd \tag{10}$$

where *Vout*(OFF) and *Vout*(ON) mean the voltages of the junction when the switch SW is off and on, respectively. The bridge sends the values of *Vout*(OFF) and *Vout*(ON) after coding them by an A/D converter on the bridge. We can know C_1 and C_2 by solving (9) and (10). The bridge has initialization process before the measurement of *Vout*(OFF) and *Vout*(ON) in which the charges in C_1, C_2 and Cref are all released.

C. LSI Chip for Bridge

At the present stage, we have completed fabrication of the first prototype of CMOS LSI based on 0.35 μm rules for the bridges (Fig. 12 a). While the size of the LSI is 5×5 mm^2, the total area of the analog-digital mixed circuits is within 1.5 mm^2. The operating frequency of the LSI is 50 MHz. Each bridge measures *Vout* with an 8-bit A/D converter and it has a function to transmit the data to the neighboring chip. We packaged the LSI on a compact (16×18 mm^2) flexible substrate (Fig. 12 b) that is folded in half (16×9 mm^2). Although this first prototype needs an additional front-end circuit IC (5×6 mm^2), the next version will not need it and can be packaged in a substrate that is almost half in size from the present one.

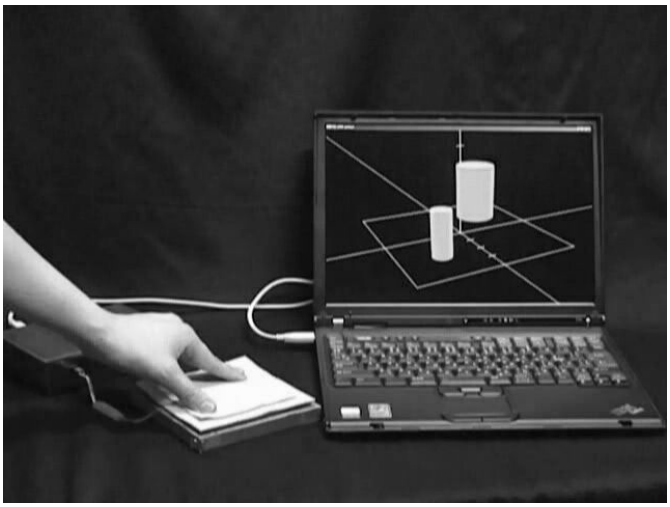

Figure 14. Demonstration. One element (near side) is pressed by the thumb, and the other (far side) is pressed by the first and second fingers. *F* and *S* (the height and the area of the base of the column) are estimated successfully.

D. Test Model of Robot Skin

We developed a test model of the sensor skin (Fig. 13) using the first prototype of the LSI. Because the protocol of the prototype is simpler than explained above, there are additional layers for signal transmission (i.e. the layer B in Fig. 2 is only used as the sensor layer). The test model is a 2×2 array and the size of each element is 40×40 mm^2. We verified that the bridges measured the capacitances of the sensor elements and the data were transmitted to the host computer successfully. In Fig. 14, we demonstrate that *F* (the height of the column) and *S* (the area of the base of the column) are estimated using the transmitted data from the bridges.

V. Conclution

In this paper, we introduced two novel technologies; the cell-bridge system and the nonlinear tactile element. The soft, stretchable, and large-area robot skin without long wires is realized by combining the two technologies.

Acknowledgment

The authors thank Naoya Asamura, Tachio Yuasa, Mitsuhiro Hakozaki, Xinyu Wang, and Hiroto Itai (Cellcross Co., Ltd.) for their cooperation on fabricating and evaluating the prototype of the CMOS LSI. We also thank Kosuke Ito and Kagari Koshi (The University of Tokyo) for their contributions on conducting the experiment and developing the test model of the sensor skin.

REFERENCES

[1] Y. Sakagami, et al, "The intelligent ASIMO: System overview and integration," Proc. of the 2002 IEEE/RSJ International Conference on Intelligent Robots and Systems (IROS 2002), vol. 3, pp. 2478-2483, 2002.

[2] K. Kaneko, et al, "Humanoid robot HRP-2," Proc. of the IEEE 2004 International Conference on Robotics and Automation (ICRA 2004), vol. 2, pp. 1083-1090, 2004.

[3] T. Shibata, K. Wada, and K. Tanie, "Tabulation and analysis of questionnaire results of subjective evaluation of seal robot in Japan, U.K., Sweden and Italy," Proc. of the IEEE 2004 International Conference on Robotics and Automation (ICRA 2004), vol. 2, pp. 1387-1392, 2004.

[4] M. Fujita, "AIBO: Toward the era of digital creatures," The International Journal of Robotics Research, vol. 20, no. 10, pp. 781-794, 2001.

[5] M. H. Lee and H. R. Nicholls, "Tactile sensing for mechatronics - a state of the art survey," Mechatronics, vol. 9, pp. 1-31, 1999.

[6] E. S. Kolesar and C. S. Dyson, "Object imaging with a piezoelectric robotic tactile sensor," IEEE Journal of Microelectromechanical Systems, vol. 4, pp. 87-96, 1995.

[7] Y. Hoshino, M. Inaba, and H. Inoue, "Model and processing of whole-body tactile sensor suit for human-robot contact interaction," Proc. of the 1998 IEEE International Conference on Robotics & Automation (ICRA '98), pp. 2281-2286, 1998.

[8] R. Kageyama, S. Kagami, M. Inaba, and H. Inoue, "Development of soft and distributed tactile sensors and the application to a humanoid robot," Proc. of the IEEE International Conference on Systems, Man, and Cybernetics, vol. 2, pp. 981-986, 1999.

[9] F. Castelli, "An integrated tactile-thermal robot sensor with capacitive tactile array," IEEE Transactions on Industry Applications, vol. 38, no. 1, pp. 85-90, 2002.

[10] O. Kerpa, K. Weiss, and H. Worn, "Development of a flexible tactile sensor system for a humanoid robot," Proc. of the 2003 IEEE/RSJ International Conference on Intelligent Robots and Systems (IROS 2003), vol. 1, pp. 1-6, 2003.

[11] M. Shimojo, A. Namiki, M. Ishikawa, R. Makino, and K. Mabuchi, "A tactile sensor sheet using pressure conductive rubber with electrical-wires stitched method," IEEE Sensors Journal, vol. 4, no. 589-596, 2004.

[12] M. Hakozaki, A. Hatori, and H. Shinoda, "A sensitive skin using wireless tactile sensing elements," Proc. of 18th Sensor Symposium, pp. 147-150, 2001.

[13] A. Okada, Y. Makino, and H. Shinoda, "Cell bridge: A signal transmission element for constructing high density sensor networks," Proc. of 2nd International Workshop on Networked Sensing Systems (INSS 2005), pp. 180-185, 2005.

[14] A. Okada, Y. Makino, and H. Shinoda, "Cell-bridge-based connection method of high density sensor elements," Proc. of 22nd Sensor Symposium, pp. 425-428, 2005.

[15] T. Hoshi and H. Shinoda, "A tactile sensing element for a whole body robot skin," Proc. of 36th International Symposium on Robotics (ISR 2005), 2005.

[16] S. Weinstein, "Intensive and extensive aspects of tactile sensitivity as a function of body part, sex, and laterality," The Skin Senses, pp. 195-222, C. C. Thomas, 1968.

[17] Y. Makino, N. Asamura, and H. Shinoda, "Multi primitive tactile display based on suction pressure control," Proc. of IEEE 12th Symposium on Haptic Interfaces for Virtual Environment and Teleoperator Systems (Haptic Symposium 2004), pp. 90-96, 2004.

[18] G. R. Strobl, The Physics of Polymers: Concepts for Understanding Their Structures and Behavior, Springer, 1997.